**iScience, Volume *24***

## Supplemental information

# Potassium ions promote hexokinase-II dependent glycolysis

**Helmut Bischof, Sandra Burgstaller, Anna Springer, Lucas Matt, Thomas Rauter, Olaf A. Bachkönig, Tony Schmidt, Klaus Groschner, Rainer Schindl, Tobias Madl, Nikolaus Plesnila, Robert Lukowski, Wolfgang F. Graier, and Roland Malli**

# Supplementary Figures and Captions

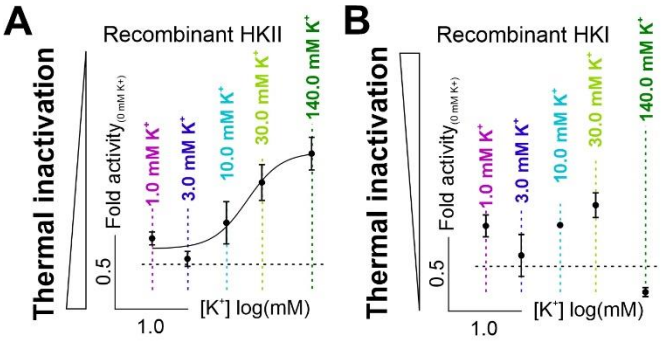


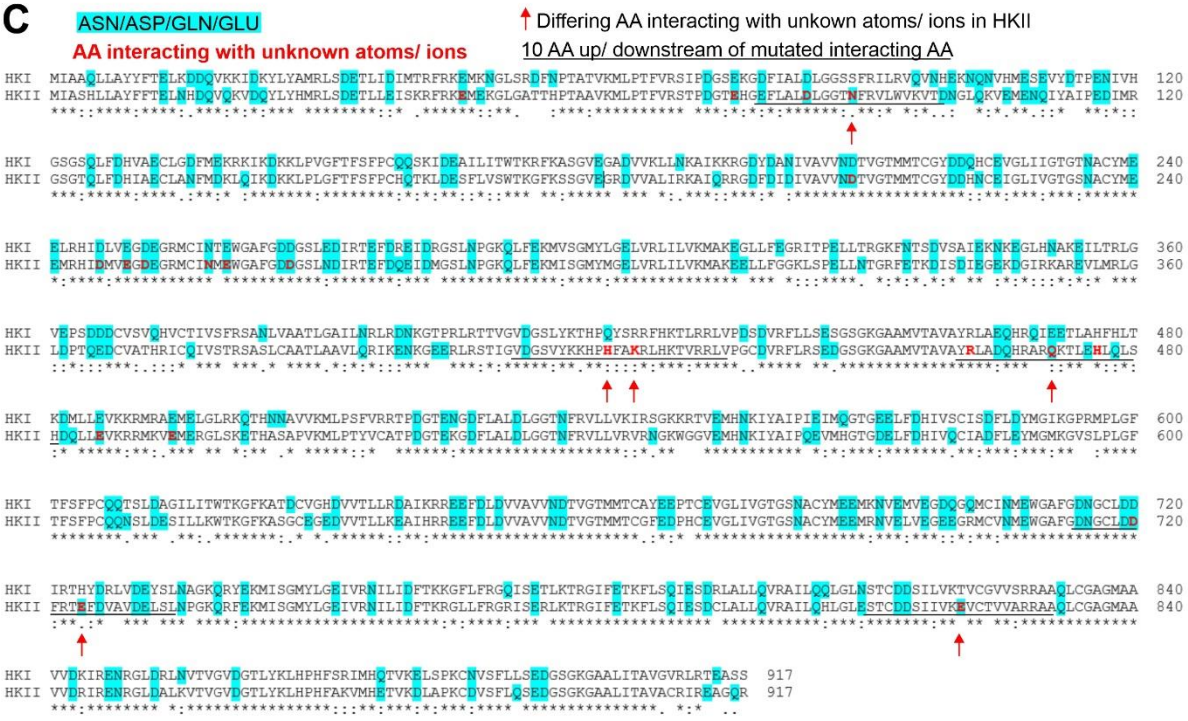


D

| Interaction site | Amino acid position | Hexokinase I | Hexokinase II |
|---|---|---|---|
| 1 | 46 | E | E |
| | 267 | D | D |
| 2 | 76 | E | E |
| | 462 | R | R |
| 3 | 84 | D | D |
| | 89 | S | N |
| 4 | 209 | D | D |
| | 258 | N | N |
| 5 | 235 | N | N |
| | 260 | E | E |
| 6 | 246 | D | D |
| | 249 | E | E |
| | 251 | D | D |
| 7 | 422 | Q | H |
| | 425 | R | K |
| 8 | 471 | E | Q |
| | 821 | T | E |
| 9 | 476 | H | H |
| | 724 | H | E |
| 10 | 486 | E | E |
| | 494 | E | E |
| | 720 | D | D |

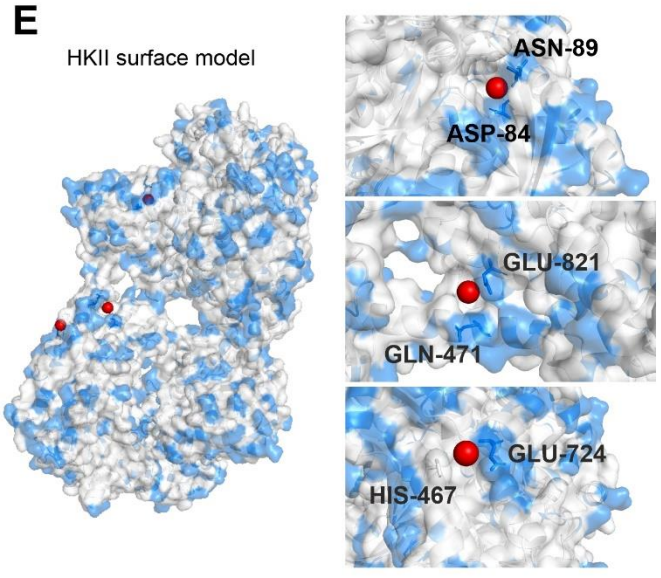


**Figure S1. Properties of HKI and HKII, related to Figure 1.** (**A, B**) Mean activity ± SEM of purified HKII (**A**) and HKI (**B**) after thermal inactivation at 37°C for 1.5 hours in the presence of different [$K^+$]. n=3 for both proteins and all [$K^+$]. (**B**) Protein sequence alignment of HKI vs. HKII. Potential $K^+$ binding

amino acids (ASN, ASP, GLN, GLU) are highlighted in blue, amino acids interacting with unknown ions or atoms in the crystal structure of HKII are written in red. Red arrows indicate a differing amino acid between HKI and HKII, which is interacting with an unknown atom or ion in HKII. Underlined regions highlight 10 amino acids up and downstream of such amino acid. (**D**) Overview of the 10 potential interaction sites as found in HKII. Interaction site (1-10), corresponding positions of the interacting amino acids and the respective amino acids found in HKI or HKII are indicated in one-letter code. Red background shows interaction sites that differ between HKI and HKII, amino acids written in red and bold highlight differing amino acids between HKI and HKII. (**E**) Surface model of HKII. Unknown atoms or ions close to the 3 interaction sites that possess a potential $K^+$ binding amino acid in HKII, but not HKI (**D**, interaction site 3, 8, 9) are shown in red.

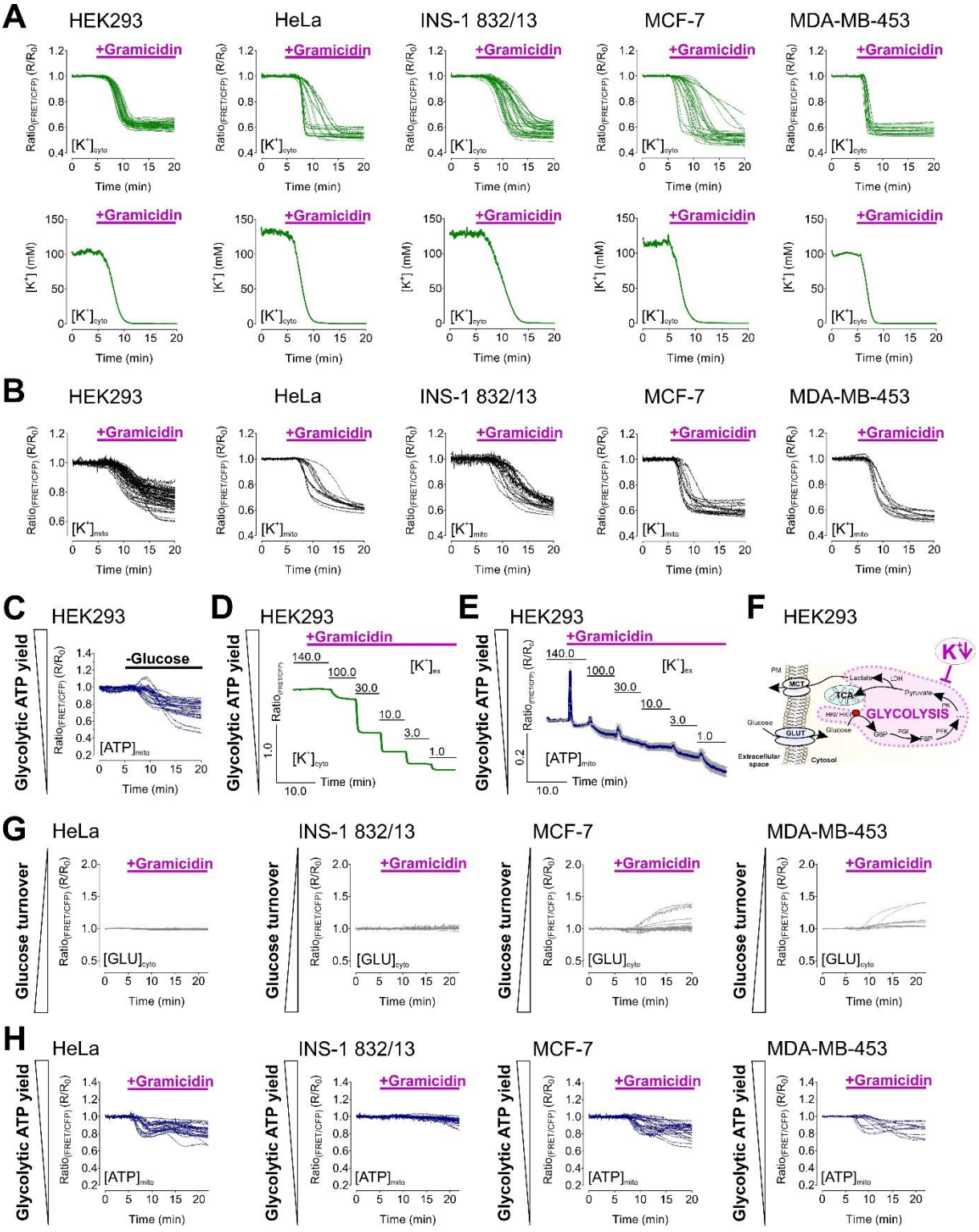


**Figure S2. Intracellular $K^+$ depletion induces disturbances of cellular energy homeostasis, related to Figure 1 and Figure 2.** (**A, B**) FRET-ratio signals over-time of HEK293 (first panel), HeLa (second panel), INS-1 832/13 (third panel), MCF-7 (fourth panel), and MDA-MB-453 cells (fifth panel), expressing NES lc-LysM GEPII 1.0 (**A**) or mt lc-LysM GEPII 1.0 (**B**), genetically encoded, FRET-based $K^+$ indicators targeted to the cytosol or the mitochondrial matrix, respectively. Lower row in (**A**) demonstrates representative $[K^+]_{cyto}$ of single cells over-time. At the time points indicated in the panels, 15 µM gramicidin were administered to the cells. Data demonstrate each single cell response. n=3 for all. (**C**) Single cell responses over-time of HEK293 cells expressing mtAT1.03 in response to the removal of extracellular glucose. n=4. (**D**) Representative single cell response of a HEK293 cell expressing NES lc-LysM GEPII 1.0 in response to treatment with gramicidin in the presence of decreasing $[K^+]_{ex}$ ranging from 140.0 mM – 1.0 mM as indicated in the panel. n=3. (**E**) $[ATP]_{mito}$ over-time of HEK293 cells in

response to gramicidin treatment, followed by decreasing $[K^+]_{ex}$ from 140.0 mM to 1.0 mM as indicated in the panel. Data shows average ± SEM of 3 independent experiments. (**F**) Schematic illustration of $K^+$ modulated metabolism. (**G, H**) FRET-ratio signals over-time of HeLa, INS-1 832/13, MCF-7 and MDA-MB-453 cells (from left to right) either expressing FLII$^{12}$Pglu-700µδ6 (**G**, grey curves) or mtAT1.03 (**H**, blue curves). At the time point indicated in the panels, 15 µM gramicidin were administered to the cells. Data demonstrate each single cell response. (**G**) n=3 for HeLa, n=4 for INS-1 832/13, n=4 for MCF-7 and n=4 for MDA-MB-453. (**H**) n=5 for HeLa, n=5 for INS-1 832/13, n=5 for MCF-7 and n=4 for MDA-MB-453.

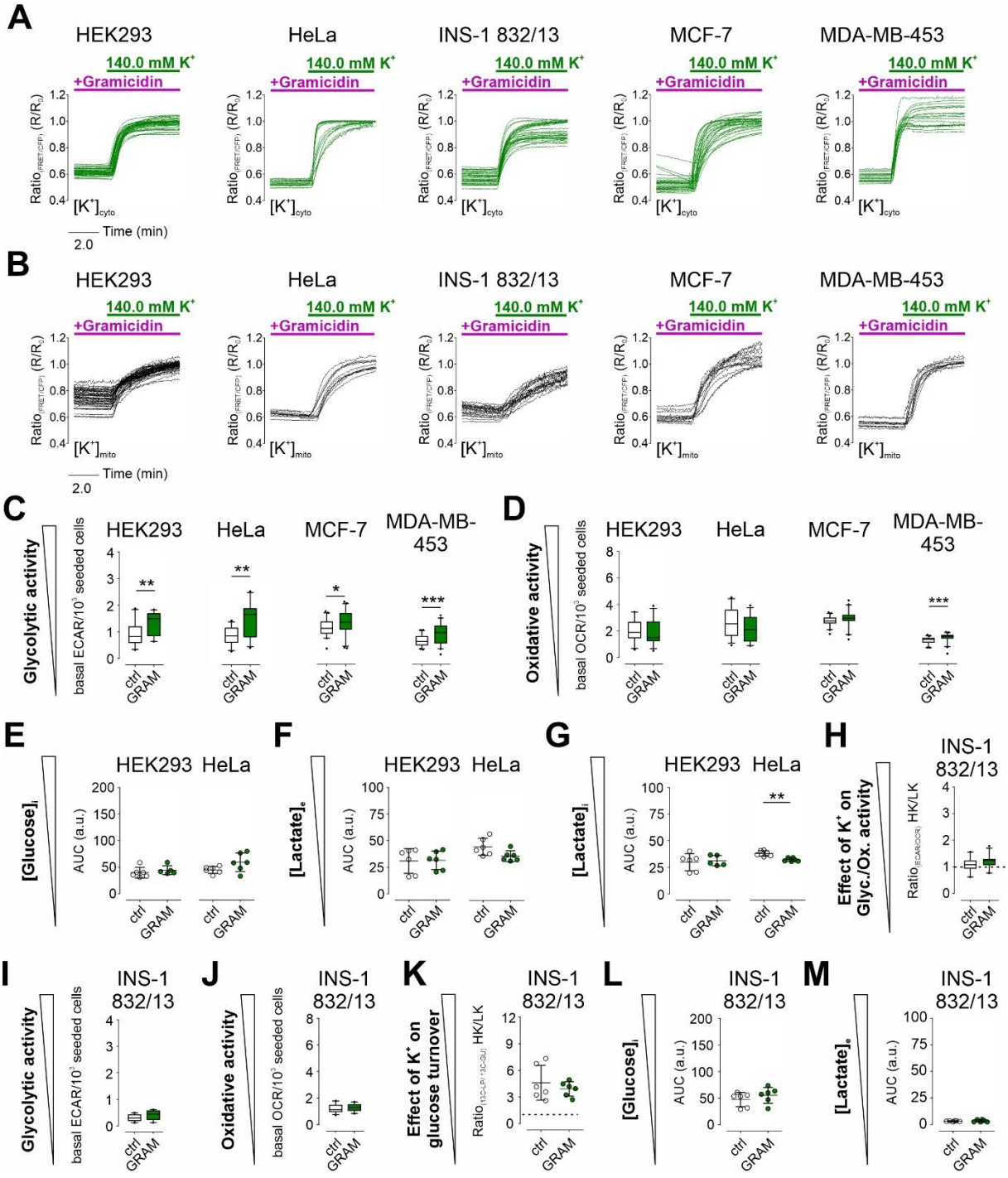


**Figure S3. Restoring high $[K^+]_i$ restores aerobic glycolysis, related to Figure 3.** (**A, B**) FRET-ratio signals over-time of different cell lines as indicated, expressing NES lc-LysM GEPII 1.0 (**A**) or mt lc-LysM GEPII 1.0 (**B**), genetically encoded, FRET-based $K^+$ indicators targeted to the cytosol or the mitochondrial matrix, respectively. Cells were treated with gramicidin in the absence of extracellular $K^+$, followed by the addition of 140.0 mM $K^+$ via a gravity-based perfusion system at time points indicated. n=3 for all. (**C, D**) Basal ECAR (**C**) and OCR (**D**) levels/$10^3$ seeded cells of (from left to right) HEK293, HeLa, MCF-7, and MDA-MB-453 cells. Cells were either treated with DMSO (ctrl, white boxes, all panels) or gramicidin (GRAM, green boxes, all panels). Boxes indicate the median and the first- and third quartile. Lower and upper whiskers indicate 5-95 percentile, outliers are indicated as black dots. n=4 for all. (**C**) *p≤0.05, **p≤0.01, ***p≤0.001 either using Unpaired t-test (HeLa and MCF-7) or Mann-Whitney test (HEK293, MDA-MB-453). (**D**) ***p≤0.001 using Mann-Whitney test. (**E-G**) Graphs show the area under the curve (AUC) of $^{13}C$-labelled glucose in the cell lysate (**E**), AUC of $^{13}C$-labelled lactate in the supernatant (**F**), or AUC of $^{13}C$-labelled lactate in the cell lysate (**G**) of HEK293 (left, all panels) or HeLa (right, all panels). Cells were either treated with DMSO (ctrl, white circles, all panels) or gramicidin

(GRAM, green circles, all panels) in the presence of 140.0 mM $K^+$. Data represent each replicate and average ± SD. n=6 for all. **p=0.0022, Mann-Whitney test. (**H-J**) Basal 140.0 mM $K^+$ (HK)/0 mM $K^+$ (LK) ECAR/OCR ratios (**H**), basal ECAR levels/$10^3$ seeded cells (**I**) and basal OCR levels/$10^3$ seeded cells (**J**) of INS-1 832/13 cells either treated with DMSO (ctrl, white boxes) or gramicidin (GRAM, green boxes) in the presence of 140.0 mM $K^+$. n=4. Boxes indicate the median and the first- and third quartile. Lower and upper whiskers indicate 5-95 percentile, outliers are indicated as black dots. (**K**) 140.0 mM $K^+$ (HK)/0 mM $K^+$ (LK) $^{13}$C-LP/$^{13}$C-GU ratios of INS-1 832/13 cells either treated with DMSO (ctrl, white circles) or gramicidin (GRAM, green circles). n=4. Data represents each replicate and average ± SD. (**L, M**) AUC of $^{13}$C-labelled glucose in the cell lysate (**L**) and AUC of $^{13}$C-labelled lactate in the supernatant (**M**) of INS-1 832/13 cells. Cells were either treated with DMSO (ctrl, white circles, both panels) or gramicidin (GRAM, green circles, both panels) in the presence of 140.0 mM $K^+$. Data shows each replicate and average ± SD, n=6 for all.

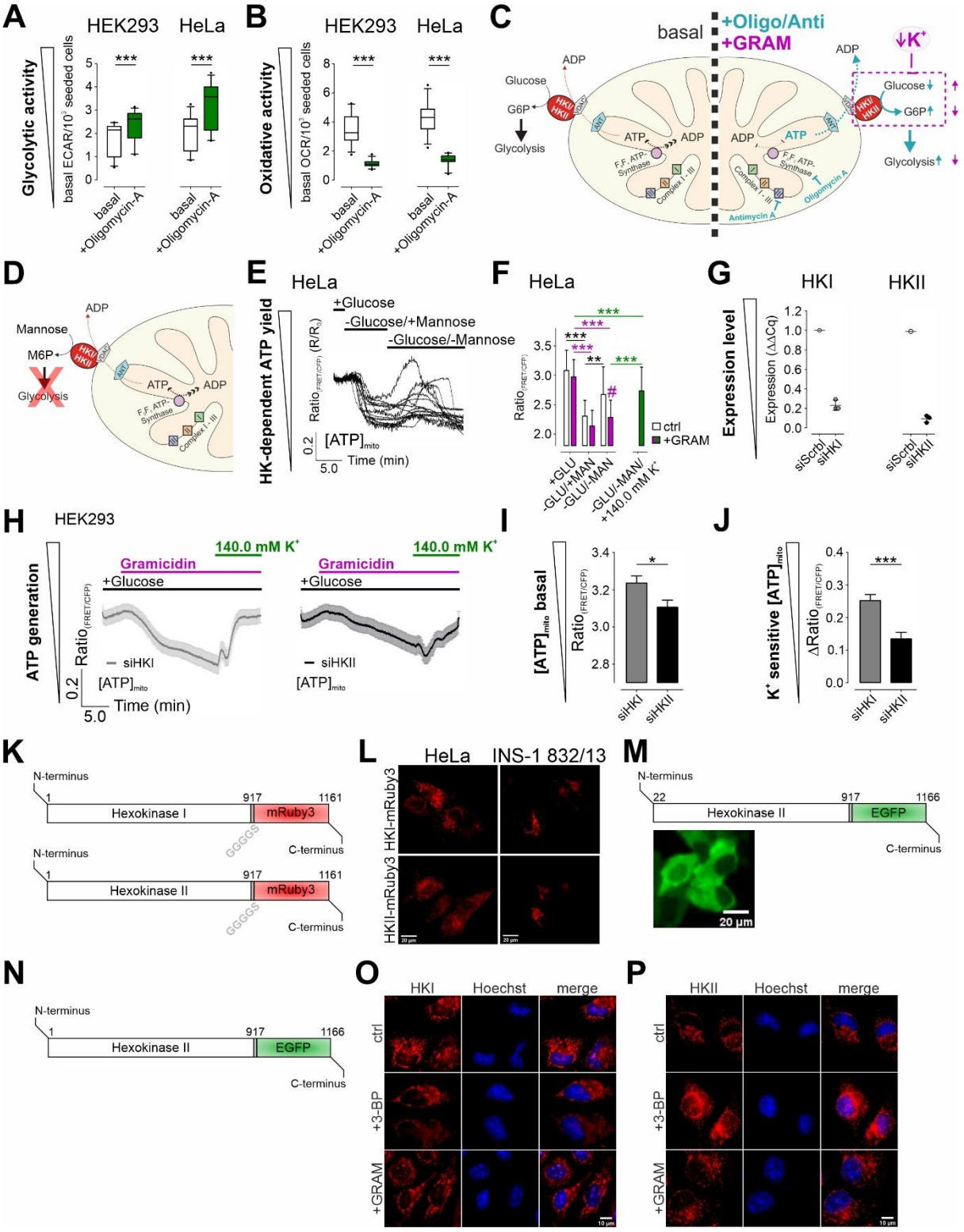


**Figure S4. HKII status determines K⁺ sensitivity of cell metabolism, related to Figure 4 and Figure 5. (A, B)** ECAR/$10^3$ seeded cells levels (**A**) and OCR/$10^3$ seeded cells (**B**) of HEK293 (left panels) and HeLa cells (right panels), either under basal conditions (basal, white boxes) or of the same cells after treatment with 2 µM oligomycin-A (+Oligomycin-A, green boxes). n=4 for all. ***p≤0.001, (**A**) Wilcoxon matched-pairs signed rank test or (**B**) Paired t-test (HEK293) and Wilcoxon matched-pairs signed rank test (HeLa). (**C**) Scheme demonstrating the first and essential step in glycolysis under basal (left), or under oligomycin-A and antimycin-A (+Oligo/Anti, cyan, right) ± gramicidin (+GRAM, magenta, right) treated conditions. (**D**) Scheme demonstrating the effect of mannose treatment on glycolysis in HeLa cells. After mannose uptake, the hexose sugar is phosphorylated to mannose-6-phosphate (M6P) by mitochondria-associated HKs, thereby consuming ATP from the mitochondrial matrix. M6P is, however,

not further utilized in glycolysis in these cells. (**E**) Single cell $[ATP]_{mito}$ responses of HeLa cells in response to mannose treatment. 10.0 mM glucose were substituted for mannose, or both hexose sugars were removed as indicated. n=4. (**F**) FRET-ratio signals of control (ctrl, white bars) or gramicidin treated HeLa cells (+GRAM, magenta and green bars) expressing mtAT1.03, either under basal conditions (+GLU), upon glucose to mannose substitution (-GLU/+MAN) and after removal of both (-GLU/-MAN). The green bar shows the FRET-ratio signal of gramicidin treated HeLa cells in the absence of both substrates upon addition of 140.0 mM $K^+$ (-GLU/-MAN/+140.0 mM $K^+$). Bars show average ± SD. Statistics correspond to the panels (**E**) and **Fig.4C**. Statistical analysis was performed either using Friedman test followed by Dunn's MC test (ctrl) or Repeated Measures One-Way ANOVA test with Geisser-Greenhouse correction, followed by Tukey's MC test (+GRAM). **p≤0.01, ***p≤0.001. #p≤0.05 using Unpaired t-test for comparison of ctrl and +GRAM under the same condition. n=4 for both. (**G**) Quantification of HKI (left) and HKII expression (right) ± SD in HEK293 cells using qPCR analysis upon cell treatment with a control siRNA (siScrbl, white circles) or siRNA against HKI (siHKI, light grey circles, left) or HKII (siHKI, dark grey circles, right), respectively. n=3 for all. (**H**) $[ATP]_{mito}$ over-time of HEK293 cells either treated with siRNA against HKI (siHKI, left panel, grey curve) or siRNA against HKII (siHKII, right panel, black curve) in response to cell treatment with 15 µM gramicidin in the absence of $K^+$, followed by re-addition of 140.0 mM $K^+$. Data represent average ± SEM, n=4 independent experiments for siHKI, n=3 independent experiments for siHKII. (**I, J**) Statistics correspond to (**H**) and demonstrate the basal FRET-ratio signal of HEK293 cells expressing mtAT1.03, either treated with siHKI (grey bars) or siHKII (black bars) (**I**), or the ΔFRET-ratio signal of mtAT1.03 upon administration of gramicidin in the absence of $K^+$, respectively (**J**). Bars show average ± SEM. n=4 for siHKI, n=3 for siHKII, *p≤0.05 using Unpaired t-test and ***p≤0.001 using Mann-Whitney test. (**K**) Schematic illustration of HKI-mRuby3 (upper scheme) and HKII-mRuby3 (lower scheme). N- and C-terminus, amino acid positions, and flexible linkers (GGGGS) are indicated. (**L**) Representative fluorescence wide-field images of HeLa (left images) and INS-1 832/13 cells (right images) either expressing HKI-mRuby3 (upper images) or HKII-mRuby3 (lower images). Scale bars show 20 µm. (**M**) Upper panel shows a schematic illustration of truncated HKII-EGFP (trHKII-EGFP), lacking the first 21 amino acids responsible for mitochondrial binding of HKII. N- and C-terminus and amino acid positions are indicated. The lower panel demonstrates representative fluorescence wide-field images of HeLa cells expressing trHKII-EGFP. Scale bar shows 20 µm. (**N**) Schematic illustration of HKII-EGFP. N- and C-terminus and amino acid positions are indicated. (**O, P**) Representative immunofluorescence wide-field images of HeLa cells stained for HKI (red, left images, **O**) or HKII (red, left images, **P**) in combination with Hoechst for nuclear staining (blue, middle images, **O** and **P**). Right images represent overlays of HKI and Hoechst (**O**) or HKII and Hoechst (**P**). HeLa cells were either not treated (ctrl, upper images, **O** and **P**) or treated with 3-BP (middle images, **O** and **P**) or gramicidin (lower images, **O** and **P**) for 15 minutes. Scale bar in the lower right images represents 10 µm. n=3 for all conditions.

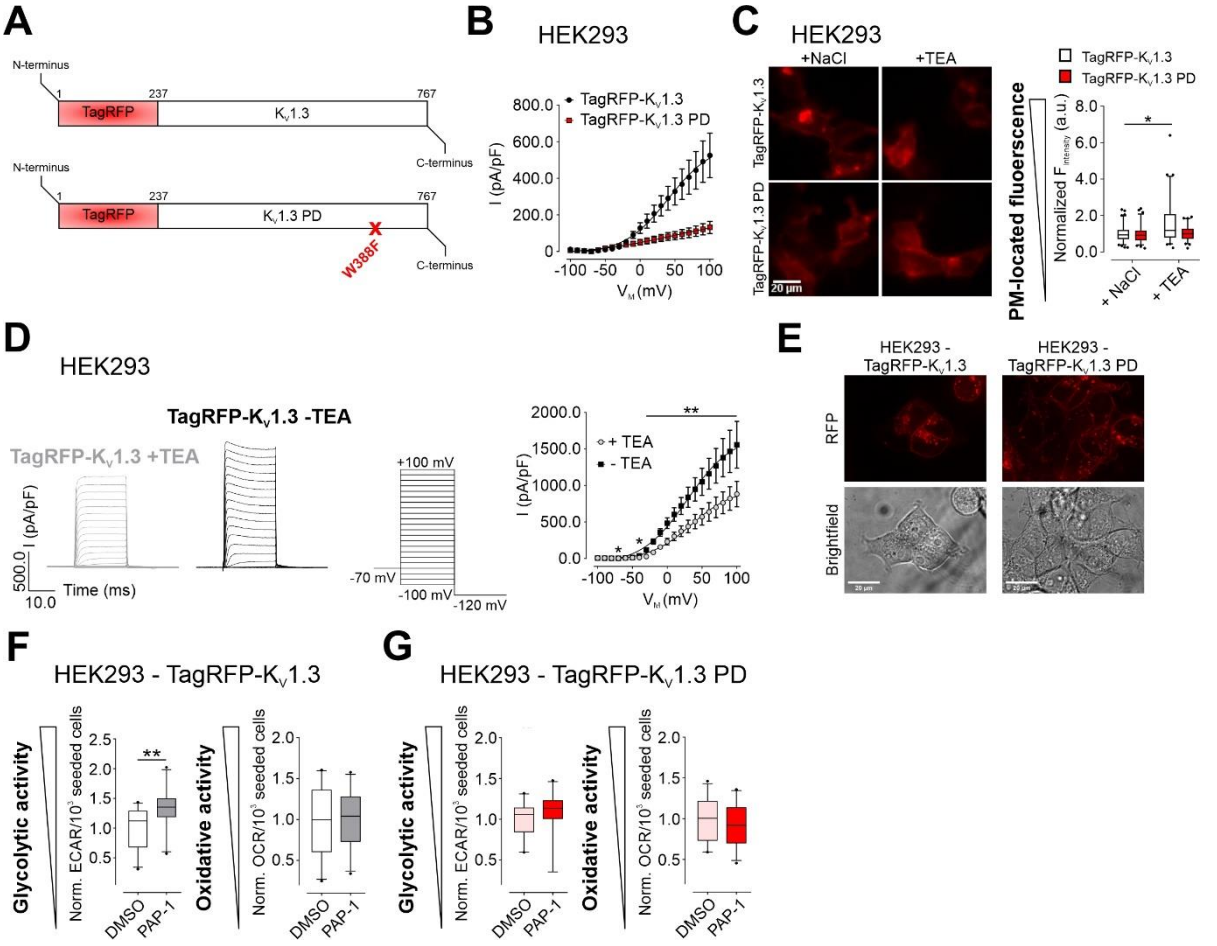


**Figure S5. Physiologic consequences of altered $K^+$ homeostasis on cell metabolism, related to Figure 6.** (**A**) Schematic representation of TagRFP-$K_V$1.3 (upper) and TagRFP-$K_V$1.3 PD (lower) bearing a W388F mutation indicated by the red X. (**B**) Current-voltage (IV) curves for TagRFP-$K_V$1.3 (black circles) and TagRFP-$K_V$1.3 PD (red squares). Data represent average ± SEM and were fitted using Boltzmann sigmoidal function. $V_{50}$ was determined as 40.60 mV (9.066 mV – 72.13 mV) for TagRFP-$K_V$1.3 and 46.28 mV (-107.90 mV – 200.40 mV) for TagRFP-$K_V$1.3 PD, respectively. n=13 HEK293 cells for TagRFP-$K_V$1.3 and n=12 HEK293 cells for TagRFP-$K_V$1.3 PD. (**C**) Representative fluorescence wide-field images (left) and quantification of plasma membrane-located fluorescence (right) in HEK293 cells either expressing TagRFP-$K_V$1.3 (upper images and white boxes) or TagRFP-$K_V$1.3 PD (lower images and red boxes). Images were acquired using 40x magnification. Cells were either cultivated in the presence of 15 mM NaCl (+NaCl, left images and boxes) or 15 mM tetraethylammonium chloride (+TEA, right images and boxes). Scale bar represents 20 µm. (**D**) Representative currents (left) and IV curves (right) of HEK293 cells expressing TagRFP-$K_V$1.3, either in the presence (TagRFP-$K_V$1.3, +TEA, grey curves and circles) or absence of TEA (TagRFP-$K_V$1.3 -TEA, black curves and circles). Currents were evoked by voltage steps as demonstrated. Data in the right panel represent average ± SEM and were fitted using Boltzmann sigmoidal function. $V_{50}$ was determined as 34.34 mV (16.66 mV – 74.90 mV) in the presence of TEA and 29.00 mV (11.16 mV – 121.20 mV) after TEA wash-out. Statistical analysis was performed either using Paired t-test (-80 mV, -70 mV, -40 mV) or Wilcoxon matched-pairs signed rank test (for all other voltages). *p≤0.05, **p≤0.01. n=9 cells. (**E**) ACLSM fluorescence (upper images) and bright-field images (lower images) of HEK293 cells either stably expressing TagRFP-$K_V$1.3 (left images) or TagRFP-$K_V$1.3 PD (right images). Scale bars represent 20 µm. (**F**) Normalized ECAR/$10^3$ (left) and OCR/$10^3$ (right) seeded HEK293 cells stably expressing TagRFP-$K_V$1.3, either in the presence of DMSO (DMSO, white boxes) or PAP-1 (PAP-1, grey boxes), in the absence of extracellular $K^+$. **p≤0.001, Unpaired t-test. n=3. (**G**) Normalized ECAR/$10^3$ (left) and OCR/$10^3$ (right) seeded HEK293 cells stably expressing TagRFP-$K_V$1.3 PD, either in the presence of DMSO (DMSO, light red boxes) or PAP-1 (PAP-1, dark red boxes), in the absence of extracellular $K^+$. p=0.1083 for ECAR and p=0.2086 for OCR, Mann-Whitney test. n=3.

## Transparent Methods

Buffers, solutions, and media

Buffers used for fluorescence time-lapse imaging comprised:
Cell equilibration buffer (in mM): 2 $CaCl_2$, 10 D-glucose, 10 HEPES, 5 KCl, 2 L-glutamine, 0.44 $KH_2PO_4$, 1 $MgCl_2$, 135 NaCl, 2.6 $NaHCO_3$, 0.34 $Na_2HPO_4$, with 1X MEM amino acids and 1X MEM vitamins added. pH was adjusted to 7.45 using NaOH.
Cytosol like buffer containing (in mM): 10 D-glucose, 0.1 EGTA, 10 HEPES, 110 KCl, 10 $MgCl_2$, 10 NaCl, pH adjusted to 7.45 with NaOH and HCl. If ions ($Ca^{2+}$, $K^+$, $Mg^{2+}$ or $Na^+$) were added or removed, NMDG in the same amount was used for osmolarity maintenance. EGTA was absent in $Ca^{2+}$ containing buffer.
0 mM $K^+$ buffer containing (in mM): 2 $CaCl_2$, with or without 10 D-glucose or D-mannose as indicated in the panels, 10 HEPES, 1 $MgCl_2$, 143 NaCl, pH adjusted to 7.45 with NaOH. In experiments where TEA was used, 15 mM of NaCl was replaced for 15 mM of TEA for osmolarity maintenance. If not otherwise stated in the panels, 0 mM $K^+$ buffer containing 2 mM $CaCl_2$ and 10 mM D-glucose was used for imaging experiments.
140.0 mM $K^+$ buffer containing (in mM): 2 $CaCl_2$, with or without 10 D-glucose or D-mannose as indicated in the panels, 10 HEPES, 140 KCl, 1 $MgCl_2$, pH adjusted to 7.45 with KOH.
To receive buffers containing different [$K^+$], 0 mM $K^+$ buffer and 140.0 mM $K^+$ buffer were mixed in appropriate portions.
For imaging experiments, gramicidin at a consistent concentration of 15 µM was used. Mitochondrial depolarization was performed using 3 µM oligomycin-A and 5 µM antimycin-A. 3-BP treatment was performed at a concentration of 300 µM. Ionomycin, nigericin, and monensin were used at a concentration of 3 µM, 5 µM, and 10 µM, respectively.

Media used for extracellular flux analysis using the Seahorse device (Agilent Technologies California, US) comprised:
SM-Na (LK) medium was composed of (in mM): 1.8 $CaCl_2$, 0.000248 $FeCl_2$, 0.814 $MgSO_4$, 115.36 NaCl, 44 $NaHCO_3$ and 0.908 $NaH_2PO_4$, with 0.5% phenol red solution, 1X MEM amino acids and 1X MEM vitamins added. Freshly, before measurements (in mM) 2 L-glutamine, 5.5 D-glucose, and 1 sodium pyruvate were added and pH was adjusted to 7.40 with NaOH.
SM-K (HK) medium was composed of (in mM): 1.8 $CaCl_2$, 0.000248 $FeCl_2$, 115.36 KCl, 44 $KHCO_3$, 0.908 $KH_2PO_4$ and 0.814 $MgSO_4$, with 0.5% phenol red solution, 1X MEM amino acids and 1X MEM vitamins added. Freshly, before measurements (in mM) 2 L-glutamine, 5.5 D-glucose, and 1 sodium pyruvate were added and pH was adjusted to 7.40 with KOH.

Buffers used for NMR sample preparation comprised:
DPBS-Na (LK) was composed of (in mM): 0.9 $CaCl_2$, with or without 10 D-glucose or $^{13}C_6$-D-glucose, 0.5 $MgCl_2$, 138 NaCl, 1.47 $NaH_2PO_4$, 15.3 $Na_2HPO_4$, with or without 0.005 PSSS, pH adjusted to 7.45 with NaOH.
DPBS-K (HK) was composed of (in mM): 0.9 $CaCl_2$, with or without 10 D-glucose or 10 $^{13}C_6$-D-glucose, 138 KCl, 1.47 $KH_2PO_4$, 15.3 $K_2HPO_4$, 0.5 $MgCl_2$, pH adjusted to 7.45 with KOH.
NMR buffer containing (in mM): 80 $Na_2HPO_4$, 5 3-(trimethylsilyl) propionic acid-2,2,3,3-d4 sodium salt (TSP) and 0.04% (w/v) $NaN_3$, all compounds were dissolved in $D_2O$ and pH was adjusted to 7.40 with NaOH and HCl.

Oligonucleotides and Plasmids

Primers used for qPCR analysis and cloning were purchased from Thermo Fisher Scientific. siRNAs used for knockdown of HKI or HKII were purchased from Santa Cruz Biotechnology (Texas, US). Scrambled siRNA was purchased from Microsynth AG (Vienna, Austria) with the following sequence: 5'–UUCUCCGAACGUGUCACGUTT–3'.
Plasmid encoding for mitochondrial-targeted ATP sensor was a gift from Hiromi Imamura at Kyoto University, Kyodai Graduate School of Biostudies, Japan.
Plasmids encoding for other genetically encoded probes except $K^+$ biosensors and $K_V$1.3 variants were purchased from Addgene: HKI-mRuby3 and HKII-mRuby3 were *de novo* synthesized and purchased from Gene Universal (Delaware, US).

Cloning and DNA purification

Cloning of TagRFP-$K_V$1.3 and TagRFP-$K_V$1.3 PD was performed using conventional PCR-, restriction- and ligation-based cloning. pGEX-MK3 served as a PCR template. For amplification of wild-type $K_V$1.3, ClaI-$K_V$1.3 fwd. and HindIII-$K_V$1.3 rev. primers were used. $K_V$1.3 W388F fwd. in combination with HindIII-$K_V$1.3 rev. and ClaI-$K_V$1.3 for., in combination with $K_V$1.3 W388F rev. primers were used to introduce the point mutation W388F in pGEX-MK3 ($K_V$1.3). PCRs were performed using Herculase II fusion DNA polymerase according to manufacturer's instructions. PCR reactions were controlled using a 1.5% agarose gel. PCR products showing the proper size after electrophoresis were cut and purified using the Wizard SV Gel and PCR Clean-Up System. The two fragments bearing the W388F mutation were used for another PCR with ClaI- $K_V$1.3 for. and HindIII $K_V$1.3 rev. primers to receive the full-length product ($K_V$1.3 PD) bearing a point mutation (W388F), followed by agarose gel electrophoresis and gel DNA extraction. Subsequently, purified PCR products of full-length $K_V$1.3 and $K_V$1.3 PD, and a pcDNA3.1(-) vector containing TagRFP were used for restriction using ClaI and HindIII according to manufacturer's instructions, followed by ligation using T4 DNA ligase. The ligated products were transformed into chemically competent 10-beta bacteria using the supplied protocol and spread on agar-agar plates containing 100 µg mL-1 ampicillin,

followed by incubation at 37°C over-night. The next day, colonies were picked, transferred into 5 mL of LB-medium with 100 µg mL-1 ampicillin added, and bacteria were cultured over-night at 37°C vigorously shaking, followed by plasmid minipreps using the Monarch Plasmid Miniprep Kit. Clones were sent for sequencing (Microsynth AG) for verification.
DNA Maxiprep's of plasmids were performed by culturing bacteria containing the respective plasmid in 500 mL LB-media, either with 100 µg mL-1 ampicillin or 50 µg mL-1 kanamycin, depending on the plasmid, over-night. The next day, plasmid DNA was extracted using the 15 NucleoBond Xtra Maxi kit according to manufacturer's instructions.

*In vitro* HK activity assay

The activity of recombinant purified HKI and HKII *in vitro* was determined using a colorimetric HK activity assay kit. To investigate thermal inactivation of HKI and HKII, 40 µL of assay buffer containing a final concentration of recombinant purified HKs of 4.0 ng/µL were incubated at 37°C for 1.5 hours. Determination of HK activities was performed using an absorbance plate reader (Infinite F200 Pro, TECAN, Männedorf, Switzerland). An average of $\Delta absorbance_{10min}$ over 1 hour was generated, and data were normalized to condition without additional $K^+$ added for representation.

*In silico* 3D modelling

3D structure of HKI and HKII were generated using the PyMol Molecular Graphics System, Version 2.0 Schrödinger, LLC., based on the crystallographic models of Rosano et al. (RCSB accession number 1QHA) for HKI and Nawaz et al. (RSCB accession number 2NZT) for HKII (Nawaz et al., 2018; Rosano et al., 1999). One asymmetric unit of the crystal structure was chosen and represented as a cartoon model in grey. Amino acids known to generate $K^+$ binding structures including asparagine, aspartate, glutamine, and glutamate were colored in blue. Unidentified atoms found in the crystallographic model of HKII are represented as red spheres.

Cell culture and transfection

HEK293, HeLa, MCF-7, and MDA-MB-453 cells (all purchased from ATCC, Virginia, US) were cultivated in DMEM (Thermo Fisher Scientific) complemented with 10% FCS, 1 mM sodium pyruvate, 100 U $mL^{-1}$ penicillin-streptomycin, and 2.5 µg $mL^{-1}$ amphotericin B. INS-1 832/13 cells were a gift from C.B. Newgard (Department of Pharmacology and Cancer Biology, Duke University School of Medicine, USA) and were cultivated in GIBCO RPMI 1640 medium additionally supplemented with 10% FCS, 10 mM HEPES, 1 mM sodium pyruvate, 0.05 mM 2-mercaptoethanol, 100 U $mL^{-1}$ penicillin-streptomycin and 2.5 µg $mL^{-1}$ amphotericin B. All cell lines were cultivated in a humidified incubator at 37°C with 5% $CO_2$. HEK293, HeLa, MCF-7 and MDA-MB-453 cells were retrieved from female organisms. INS-1 832/13 cells were retrieved from a male organism. HeLa cells were authenticated by STR analysis. All other cell lines were not authenticated.

For transfection, either PolyJet *in vitro* DNA transfection reagent (SignaGen Laboratories, Maryland, US) or TransFast transfection reagent (Promega GmbH) were used according to manufacturer's instructions.

Extracellular flux analysis

Assessment of OCR and ECAR levels was performed using a Seahorse-XFe96 Analyzer (Agilent Technologies). For analysis of wild-type cells, cells were seeded one day before the experiment in the respective cell culture medium using the following cell numbers: 70,000, 50,000, 100,000, 50,000, and 80,000 cells for HEK293, HeLa, INS-1 832/13, MCF-7, and MDA-MB-453 cells, respectively. Cells were cultivated over-night in a humidified incubator at 37°C and 5% $CO_2$. The next day, cells were removed from the incubator and washed 2X with SM-Na (LK) or SM-K (HK) medium, prior SM-Na/K medium containing 5 µM gramicidin (1:3,000 from DMSO stock) or 0.033% DMSO was added. Subsequently, cells were incubated at ambient environment at 37°C for 20 minutes, 5 µM gramicidin or 0.033% DMSO containing medium was removed and replaced for the respective SM-Na/SM-K medium, followed by a 10-minute incubation phase at 37°C. Next, cells were analyzed using the Seahorse-XFe96 Analyzer (Agilent Technologies).

For analysis of ECAR- and OCR levels under conditions of mitochondrial inhibition, oligomycin-A at a final concentration of 2 µM (1:1,000 from DMSO stock) was injected. Either ECAR/OCR ratio was calculated, or ECAR and OCR raw values were normalized for the seeded cell numbers.

For extracellular flux analysis of HEK293 cells stably expressing TagRFP-$K_V$1.3 or TagRFP-$K_V$1.3 PD, cells originally cultivated in the presence of 1 µM PAP-1 (1:10,000 from DMSO stock) were pelleted at 200 rcf at room temperature for 5 minutes, the supernatant was removed, cells were resuspended in complemented DMEM without PAP-1 and re-pelleted at 200 rcf at room temperature for 5 minutes. Again, the supernatant was removed, cells were resuspended in fresh complemented DMEM without PAP-1 and were seeded at 70.000 cells per well in complemented DMEM, either in the presence of 1 µM PAP-1 (1:10,000 from DMSO stock) or equivalent amounts of DMSO (0.01%). Cells were cultivated over-night in a humidified incubator at 37°C in the presence of 5% $CO_2$. The next day, cells were removed from the incubator and washed 1X with SM-Na (LK) or SM-K (HK) medium with 1 µM PAP-1 (1:10,000 from DMSO stock) or equivalent levels of DMSO (0.01%), respectively. Subsequently, cells were incubated in an ambient environment at 37°C for 30 minutes and cells were analyzed using the Seahorse-XFe96 Analyzer (Agilent Technologies). ECAR as well as OCR values were normalized for the seeded cell number, or ECAR/OCR levels were calculated. All data were analyzed using Seahorse Wave Desktop Software (Agilent Technologies) and Microsoft Excel software (Microsoft, New Mexico, US).

Determination of the $K^+$ sensitivity of $[ATP]_{mito}$ and $[GLU]_{cyto}$

$EC_{50}$ of $[ATP]_{mito}$ for $K^+$ was assessed using HEK293 cells expressing mtAT1.03. Analysis was performed using an fluorescence microscope as specified in the "Wide-field fluorescence time-lapse imaging" section. Experiments were started in the presence of 140.0 mM $K^+$ buffer followed by gramicidin administration. Subsequently, $[K^+]$ was reduced to 1.0 mM $K^+$ as indicated in the panels. For analysis, normalized FRET-ratio, i.e. $[ATP]_{mito}$, was plotted over the respective $[K^+]$ present in the extracellular buffer.

$EC_{50}$ of $[GLU]_{cyto}$ for $K^+$ was assessed using HEK293 cells expressing FLII$^{12}$Pglu-700µδ6. Therefore, 30.000 HEK293 cells were seeded per well of a black 96-well cell culture microplate with transparent bottom two days before the experiment. After 24 hours, cells were transfected with FLII$^{12}$Pglu-700µδ6 using PolyJet transfection reagent according to manufacturer's instructions. The next day, media was removed, cells were washed once with 0 mM $K^+$ buffer, followed by an incubation for 20 minutes with buffers containing different $[K^+]$ received from mixing 0 mM $K^+$ buffer and 140.0 mM $K^+$ buffer in appropriate portions, and 15 µM gramicidin. After 20 minutes, FRET-ratio signals were analyzed using the CLARIOstar fluorescence plate-reader (BMG Labtech, Ortenberg, Germany). For analysis, the normalized FRET-ratio, i.e. $[GLU]_{cyto}$, was plotted over the respective $[K^+]$ present in the extracellular buffer.

Metabolite quantification using NMR

For NMR-experiments, HEK293, HeLa, and INS-1 832/13 cells were cultivated in 10 cm dishes using the respective culture medium. At a confluence of ~80% the medium was removed, and cells were washed with DPBS-Na/DPBS-K medium containing 10 mM D-glucose and 5 µM PSSS for extracellular $K^+$ removal. Subsequently, cytosolic glucose of cells was depleted by changing medium to DPBS-Na/DPBS-K without D-glucose, with 5 µM PSSS added. After an incubation phase of 5 minutes, DPBS-Na/DPBS-K medium without D-glucose and without PSSS, either containing 15 µM gramicidin (1:1,000 from DMSO stock) or 0.1% DMSO were added, and after 5 minutes cell supernatant was exchanged for the same medium. After another 15 minutes, DPBS-Na/DPBS-K containing $^{13}C_6$-labelled glucose was added for 20 minutes and 0.5 mL of supernatant was collected for later analysis. Cells were quickly washed 1X with DPBS-Na/DPBS-K medium without D-glucose and without $^{13}C_6$-labelled glucose, media was removed, 0.5 mL of ddH2O was added, cells were scraped using cell scrapers and the lysate was transferred into 2.0 mL reaction tubes. For protein removal and to quench enzymatic reactions in the samples, the 0.5 mL of each sample was mixed with 1.0 mL of methanol, and samples were homogenized using a precellys homogenizer. Both, media and cell pellets, were stored at -20°C for 1 hour until further processing. Afterwards, the samples were spun at 17949 rcf at 4°C for 30 minutes. Supernatants were lyophilized and 0.5 mL of NMR buffer was added to the samples and transferred to 5 mm NMR tubes. All NMR

experiments were performed at 310 K on an AVANCE™ Neo Bruker Ultrashield 600 MHz spectrometer equipped with a TXI probe head and processed as described previously (Alkan et al., 2018). The 1D CPMG (Carr-Purcell_Meiboom_Gill) pulse sequence (cpmgpr1d, 512 scans, 73728 points in F1, 11904.76 Hz spectral width, 128/512 transients for media/cell extracts, recycle delays 4 s) with water suppression using pre-saturation, was used for $^{1}$H 1D NMR experiments. Bruker Topspin version 4.0.2 was used for NMR data acquisition. The spectra for all samples were automatically processed (exponential line broadening of 0.3 Hz), phased, and referenced using TSP at 0.0 ppm using Bruker Topspin 4.0.2 software (Bruker GmbH, Rheinstetten, Germany). Spectra pre-processing and data analysis have been carried out using the state-of-the-art data analysis pipeline proposed by the group of Prof. Jeremy Nicholson at Imperials College London using Matlab® scripts and MetaboAnalyst 4.0 (Chong et al., 2018). NMR data were imported to Matlab® vR2014a (Mathworks, Natick, Massachusetts, United States), regions around the water, TSP, and remaining methanol signals excluded, and probabilistic quotient normalization (Dieterle et al., 2006) was performed to correct for sample metabolite dilution. To identify changes in metabolic profiles, multivariate statistical analysis was performed as described previously(Huber et al., 2019) and includes Principle Component Analysis (PCA), Orthogonal-Partial Least Squares - Discriminant Analysis (O-PLS-DA) (Maher et al., 2008), and all associated data consistency checks and 7-fold cross-validation. Stated concentrations correspond to normalized concentrations after probabilistic quotient normalization.

Wide-field fluorescence time-lapse imaging

Prior to experiments, all cells were equilibrated for at least 30 minutes in cell equilibration buffer. Time-lapse imaging experiments of cells was performed either using an Olympus IX73 inverted microscope (Olympus, Vienna, Austria) with a 40X objective (UApo N 340, 40X/1.35 Oil, ∞/0.17/FN22, Olympus), or a Zeiss Axiovert.A1 FL (Zeiss, Oberkochen, Germany) equipped with a 40X objective (Objectiv Fluar, 40X/1,30 Oil M27, Zeiss). Both microscopes were connected to an OMICRON LedHUB High-Power LED Light Engine for illumination, equipped with a 455 nm and either a 530 nm or a 505-600 nm LED light source (OMICRON electronics, Vienna, Austria). Excitation filters were as follows: 427/10 nm and 575/15 (AHF Analysentechnik, Tübingen, Germany), respectively. Emission of FRET-sensors was detected at 475 and 530 nm, respectively, and emissions were either separated using a photometrics DV2 image splitter (Teledyne Technologies Inc., Arizona, US), or an Optosplit II image splitter (Teledyne Technologies Inc.), both equipped with a T505lpxr (AHF Analysentechnik) . Images were captured at a binning of 4, either using a Retiga R1 CCD-camera (TELEDYNE QIMAGING, Surrey, Canada) attached to the Olympus IX73, or a pco.panda 4.2 bi sCMOS-camera (PCO, Kelheim, Germany) attached to the Zeiss Axiovert.A1 FL. Buffer exchange and cell stimulation during data acquisition were performed using the PC30 perfusion chamber

(NGFI GmbH, Graz, Austria) connected to a gravity-based perfusion system (NGFI GmbH). For data analysis, raw fluorescence over-time values were exported to Microsoft Excel software (Microsoft) corrected for the background, and FRET-ratio values were generated

High-resolution confocal imaging

Array Confocal microscopy was performed using an array confocal laser scanning microscope (ACLSM) built on a fully automatic inverse microscope (Axio Observer.Z1, Zeiss) using a 100X objective (Plan-Apochromat 100X, 1.4 Oil M27, Zeiss). Microscope was equipped with a Yokogawa CSU-X1 Nipkow spinning disk system and a piezoelectric z-axis motorized stage. Laser light of diode lasers (Visitron Systems) served as excitation light source: GFP of HKII was excited using a 488 nm laser light, mRuby3 of HKI and TagRFP-$K_V$1.3 variants was excited using 561 nm laser light. Emissions were captured at 516 nm and 644 nm, respectively. The VisiView Premier Acquisition software (Visitron Systems, Puchheim, Germany) was used for image acquisition and microscope control. Buffer exchange and cell stimulation during data acquisition was performed using the PC30 perfusion chamber (NGFI GmbH) connected to a gravity-based perfusion system (NGFI GmbH). Image representation of ACLSM images and analysis of cytosolic HKII-GFP/HKI-RFP ratio was performed using ImageJ and Microsoft Excel software.

qPCR analysis

Expression levels of HKI and HKII were assessed on day 2 after siRNA transfection. RNAs were isolated using the peqGOLD total-RNA kit and cDNA was generated using the High-Capacity cDNA Reverse Transcription Kit according to manufacturer's instructions. qRT-PCR was performed using the GoTaq qPCR Kit on a LightCycler 480 (Roche Diagnostics, Vienna, Austria). Relative expression of specific genes was normalized to $\alpha$-Tubulin as a housekeeper.

Generation of HEK293 cells stably expressing TagRFP-$K_V$1.3 or TagRFP-$K_V$1.3 PD

HEK293 cells were transfected with respective plasmids using PolyJet transfection reagent. 48 hours after transfection, G418 at a final concentration of 500 µg $\mu L^{-1}$ was added. After 5 days of cell cultivation in the presence of G418, cells were detached, sorted by FACS (FACS Aria IIIu, BD Biosciences, Heidelberg, Germany) for red fluorescence (excitation at 561 nm, emission 586/15 nm) and mixed cell populations of each $K_V$1.3 variant were cultivated.

Immunofluorescence staining and quantification

On day of fixation, cells were washed 2X with PBS, and fixed using a 50/50 mixture of -18°C cooled methanol/ acetone followed by washing 3X with PBS and addition of the blocking buffer (5% BSA in PBS) for 2 hours mildly shaking. Subsequently, primary antibodies (Mouse monoclonal anti-$\alpha$-Tubulin, RRID: AB_1904178, Rabbit monoclonal anti-Hexokinase I, RRID: AB_2116996, Rabbit monoclonal anti-Hexokinase II, RRID: AB_2232946) were added to the

cells in PBS with 5% BSA. Cells were incubated over-night at 4°C. On the next day, primary antibody solutions were removed, cells were washed 3x with blocking buffer and secondary antibody solution containing Goat anti-Mouse IgG1 Cross-Adsorbed Secondary Antibody, Alexa Fluor 488 (RRID: AB_2535764) and Goat anti-Rabbit IgG (H+L) Cross-Adsorbed Secondary Antibody, Alexa Fluor 555 (RRID: AB_2535849) at a dilution of 1:2,500 were added. Cells were incubated for 2 hours in the dark at room temperature. Finally, cells were washed 3X with PBS, and mounted using PermaFluor Aqueous Mounting Medium with 1 µg $mL^{-1}$ Hoechst 33342 added. Images were acquired using a Zeiss Axiovert.A1 FL equipped with a 40X objective (Objectiv Fluar, 40X/1,30 Oil M27, Zeiss). For illumination, an OMICRON LedHUB High-Power LED Light Engine equipped with a 385 nm, 475 nm, and 505-600 nm LED (OMICRON electronics), and 380x, 473/10, and 575/15 excitation filters (all from AHF Analysentechnik), was used.

For investigation of endogenous HKI and HKII localizations upon 3-BP or gramicidin treatment, cells were treated at room temperature with 500 µM 3-BP or 15 µM gramicidin in 0 mM $K^+$ buffer for 15 minutes prior to fixation.

Patch-clamp recordings

Recordings were performed in whole-cell mode. Currents were evoked by 21 voltage square pulses (20 ms each) from -70 mV holding potential to voltages between -100 mV and +100 mV delivered in 10 mV increments. Voltages were corrected off-line for the capacity referring to the surface of the plasma membrane. The pipette solution contained (in mM): 0.05 EGTA, 10 HEPES, 110 K-Aspartate, 30 KF, 1 $MgCl_2$ and 10 NaCl, pH adjusted to 7.20 with KOH. For amplifier control and data acquisition, Patchmaster software (HEKA Elektronik GmbH, Lambrecht, Germany) was used. Data analysis was performed using Fitmaster software (HEKA Elektronik GmbH), Nest-o-Patch software (http://sourceforge.net/projects/nestopatch, written by Dr. V Nesterov), and Microsoft Excel (Microsoft).

Statistical analysis

Statistical analysis was performed using Prism5 software (GraphPad). Data were tested for Gaussian distribution using D'Agostino and Pearson omnibus normality test. Either a two-tailed Unpaired t-test or a two-tailed Mann-Whitney test was used for pairwise comparison of non-paired observations. For pairwise comparison of paired observations, either a Paired t-test or Wilcoxon matched-pairs signed rank test was used. Comparison of >2 data sets was done either using One-way ANOVA followed by Tukey's multiple comparison (MC) test, Repeated Measures ANOVA followed by Tukey's MC test, Kruskal-Wallis test followed by Dunn's MC test or Friedman test followed by Dunn's MC test. The statistical test is indicated in the figure legends. p-values of ≤0.05 were indicated with *, p≤0.01 with **, and p≤0.001 with ***. No sample size estimation was performed.

## Supplemental References


Alkan, H.F., Walter, K.E., Luengo, A., Madreiter-Sokolowski, C.T., Stryeck, S., Lau, A.N., Al-Zoughbi, W., Lewis, C.A., Thomas, C.J., Hoefler, G., et al. (2018). Cytosolic Aspartate Availability Determines Cell Survival When Glutamine Is Limiting. Cell Metabolism *28*, 706-720.e6.

Chong, J., Soufan, O., Li, C., Caraus, I., Li, S., Bourque, G., Wishart, D.S., and Xia, J. (2018). MetaboAnalyst 4.0: towards more transparent and integrative metabolomics analysis. Nucleic Acids Research *46*, W486–W494.

Dieterle, F., Ross, A., Schlotterbeck, G., and Senn, H. (2006). Probabilistic Quotient Normalization as Robust Method to Account for Dilution of Complex Biological Mixtures. Application in $^{1}$H NMR Metabonomics. Anal. Chem. *78*, 4281–4290.

Huber, K., Hofer, D.C., Trefely, S., Pelzmann, H.J., Madreiter-Sokolowski, C., Duta-Mare, M., Schlager, S., Trausinger, G., Stryeck, S., Graier, W.F., et al. (2019). N-acetylaspartate pathway is nutrient responsive and coordinates lipid and energy metabolism in brown adipocytes. Biochimica et Biophysica Acta (BBA) - Molecular Cell Research *1866*, 337–348.

Maher, A.D., Crockford, D., Toft, H., Malmodin, D., Faber, J.H., McCarthy, M.I., Barrett, A., Allen, M., Walker, M., Holmes, E., et al. (2008). Optimization of Human Plasma $^{1}$H NMR Spectroscopic Data Processing for High-Throughput Metabolic Phenotyping Studies and Detection of Insulin Resistance Related to Type 2 Diabetes. Anal. Chem. *80*, 7354–7362.

Nawaz, M.H., Ferreira, J.C., Nedyalkova, L., Zhu, H., Carrasco-López, C., Kirmizialtin, S., and Rabeh, W.M. (2018). The catalytic inactivation of the N-half of human hexokinase 2 and structural and biochemical characterization of its mitochondrial conformation. Bioscience Reports *38*, BSR20171666.

Rosano, C., Sabini, E., Rizzi, M., Deriu, D., Murshudov, G., Bianchi, M., Serafini, G., Magnani, M., and Bolognesi, M. (1999). Binding of non-catalytic ATP to human hexokinase I highlights the structural components for enzyme–membrane association control. Structure *7*, 1427–1437.